HHS Public Access

Author manuscript

Cell Rep. Author manuscript; available in PMC 2015 July 15.

Published in final edited form as:

Cell Rep. 2015 May 19; 11(7): 1031–1042. doi:10.1016/j.celrep.2015.04.021.

Differential Connexin Function Enhances Self-Renewal in Glioblastoma

Masahiro Hitomi[1,2,9], **Loic P. Deleyrolle**[3,9], **Erin E. Mulkearns-Hubert**[1], **Awad Jarrar**[1], **Meizhang Li**[1,10], **Maksim Sinyuk**[1], **Balint Otvos**[1], **Sylvain Brunet**[4], **William A. Flavahan**[5], **Christopher G. Hubert**[5], **Winston Goan**[1], **James S. Hale**[1], **Alvaro G. Alvarado**[1,2], **Ao Zhang**[1], **Mark Rohaus**[3], **Muna Oli**[3], **Vinata Vedam-Mai**[3], **Jeff M. Fortin**[3], **Hunter S. Futch**[3], **Benjamin Griffith**[3], **Qiulian Wu**[5], **Chunhong Xia**[6], **Xiaohua Gong**[6], **Manmeet S. Ahluwalia**[7,8], **Jeremy N. Rich**[2,5,7,8], **Brent A. Reynolds**[3,*], and **Justin D. Lathia**[1,2,7,8,*]

[1]Department of Cellular and Molecular Medicine, Lerner Research Institute, Cleveland Clinic, Cleveland, OH 44915, USA

[2]Molecular Medicine, Cleveland Clinic Lerner College of Medicine, Case Western Reserve University, Cleveland, OH 44195, USA

[3]Department of Neurosurgery, University of Florida, Gainesville, FL 32610-0261, USA

[4]Department of Neurosciences, Lerner Research Institute, Cleveland Clinic, Cleveland, OH 44915, USA

[5]Department of Stem Cell Biology and Regenerative Medicine, Lerner Research Institute, Cleveland Clinic, Cleveland, OH 44915, USA

[6]Berkeley Stem Cell Center, University of California, Berkeley, Berkeley, CA 94720, USA

[7]Rose Ella Burkhardt Brain Tumor and Neuro Oncology Center, Cleveland Clinic, Cleveland, OH 44195, USA

[8]Case Comprehensive Cancer Center, Cleveland, OH 44106, USA

SUMMARY

The coordination of complex tumor processes requires cells to rapidly modify their phenotype and is achieved by direct cell-cell communication through gap junction channels composed of

[*]Correspondence: brent.reynolds@neurosurgery.ufl.edu (B.A.R.), lathiaj@ccf.org (J.D.L.), http://dx.doi.org/10.1016/j.celrep.2015.04.021.

[9]Co-first author

[10]Present address: Laboratory of Biochemistry and Molecular Biology, School of Life Sciences, Yunnan University, Kunming 650091, China

SUPPLEMENTAL INFORMATION

Supplemental Information includes Supplemental Experimental Procedures and three figures and can be found with this article online at http://dx.doi.org/10.1016/j.celrep.2015.04.021.

AUTHOR CONTRIBUTIONS

M.H., L.P.D., E.E.M.-H., A.J., B.A.R., and J.D.L. conceived and designed the study. B.A.R. and J.D.L. provided financial support. M.H., L.P.D., E.E.M.-H., A.J., M.L., M.S., B.O., S.B., W.A.F., C.G.H., W.G., J.S.H., A.G.A., A.Z., M.R., M.O., V.V.-M., J.M.F., H.S.F., B.G., Q.W., C.X., and X.G. collected and/or assembled the data. M.H., L.P.D., E.E.M.-H., A.J., S.B., M.S.A., J.N.R., B.A.R., and J.D.L. analyzed and interpreted the data. M.H., L.P.D., E.E.M.-H., B.A.R., and J.D.L. wrote the manuscript. All authors gave final approval of the manuscript.

connexins. Previous reports have suggested that gap junctions are tumor suppressive based on connexin43 (Cx43), but this does not take into account differences in connexin-mediated ion selectivity and intercellular communication rate that drive gap junction diversity. We find that glioblastoma cancer stem cells (CSCs) possess functional gap junctions that can be targeted using clinically relevant compounds to reduce self-renewal and tumor growth. Our analysis reveals that CSCs express Cx46, while Cx43 is predominantly expressed in non-CSCs. During differentiation, Cx46 is reduced, while Cx43 is increased, and targeting Cx46 compromises CSC maintenance. The difference between Cx46 and Cx43 is reflected in elevated cell-cell communication and reduced resting membrane potential in CSCs. Our data demonstrate a pro-tumorigenic role for gap junctions that is dependent on connexin expression.

Graphical abstract

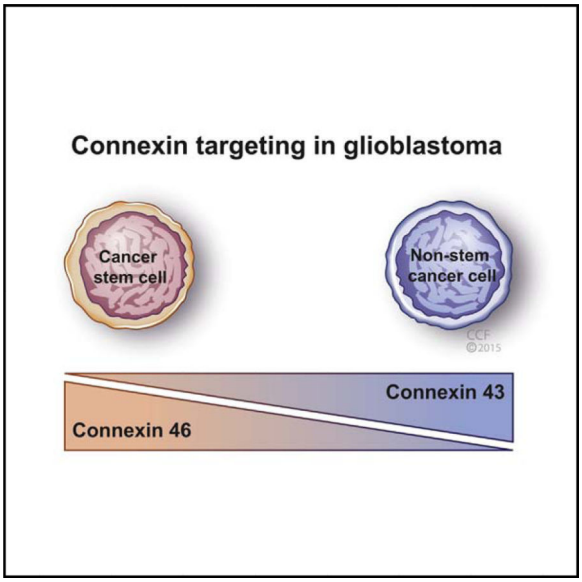

INTRODUCTION

Glioblastoma (GBM) is the most common primary malignant brain tumor and remains uniformly fatal despite aggressive therapies including surgery, radiation, and chemotherapy (Stupp et al., 2009). Many barriers to effectively treating GBM exist and include the development of therapeutic resistance and inter- and intra-tumor heterogeneity. While there is an ongoing effort to identify key molecular alterations driving GBM, targeted therapies based on these events have not effectively translated into patient survival benefits. GBM possesses a high degree of cellular heterogeneity and contains self-renewing, tumorigenic cancer stem cells (CSCs) that contribute to tumor propagation (Galli et al., 2004; Ignatova et al., 2002; Singh et al., 2003, 2004)and therapeutic resistance (Bao et al.,2006; Liu et al., 2006). The integration of CSCs into tumor models presents an opportunity to develop more effective GBM therapies, and CSC-directed therapies have shown promise in pre-clinical studies.

CSC interactions with the surrounding microenvironment dictate the balance between self-renewal and differentiation via growth factors, extracellular matrix, and communication with adjacent cells (Visvader and Lindeman, 2012). Direct cell-cell communication synchronizes groups of cells to execute coordinated programs required for growth, differentiation, and therapeutic response (Naus and Laird, 2010). The rapid diffusion of essential signaling molecules, such as cyclic AMP, inositol 1,4,5-tri-phosphate, ions, and nutrients between adjacent cells, is facilitated by gap junctions (Evans and Martin, 2002). Gap junctions are formed by six connexin subunits that assemble at the interface between adjacent cells, allowing direct cell-cell communication for molecules less than 1 kDa in size. The connexin family contains over 20 proteins with tissue-specific expression and function that are named according to predicted molecular weight. Diversity in connexin expression is responsible for differentialion permeability and varying diffusion rates (Elfgang et al., 1995; Lin et al., 2004). Switching of connexin subunits occurs during development as a result of changes required during tissue maturation (Banerjee et al., 2011), i.e., transitioning from a stem cell to a differentiated state. Connexin function is required for normal physiology, and dysfunction in connexins has been linked to a variety of disorders, including deafness (connexin 26 [Cx26]) (Gerido et al., 2007), peripheral neuropathy (Cx32) (Scherer and Kleopa, 2012), and cataracts (Cx46 and Cx50)(Beyer and Berthoud, 2014).

One of the most extensively studied connexins is Cx43, which has served as a paradigm for gap junction function during development and disease. Cx43 is essential for neural progenitor cell (NPC) proliferation and self-renewal (Cheng et al., 2004; Elias et al., 2007), but is decreased in GBM compared with lower grade tumors (Soroceanu et al., 2001). CSCs express low levels of Cx43, and overexpression of Cx43 in CSCs increased GBM latency (Yu et al., 2012). Similar findings in other advanced cancers have served as a basis for the hypothesis that gap junctions act as tumor suppressors (Kandouz and Batist, 2010). However, this role for gap junctions fails to model the connexin diversity driving communication rate and ion specificity in a cell-type-dependent manner (Evans and Martin, 2002). Based on the elevated cellular density in GBM, which increases the opportunity for direct cell communication, and the dependence of CSC maintenance on cell-cell interactions, we interrogated the function of connexins in GBM. While previous reports suggest that gap junctions have a tumor-suppressive function, we now report that gap junctions are essential for GBM growth. We identified Cx46 as enriched in CSCs and essential for their maintenance and negatively correlating with GBM patient survival. Our data support a model where the tumor-promoting function of gap junctions is dependent on the composition of connexin subunits and impacts intercellular communication, resting membrane potential, and CSC maintenance.

RESULTS

Gap Junctions Are Present in GBM and CSCs

Previous work in GBM demonstrated a tumor-suppressive role for gap junctions based on reduced expression of Cx43 in GBM (Soroceanu et al., 2001) and CSCs (Yu et al., 2012). Given the importance of CSCs for tumor progression, we sought to determine whether gap junctions were present and functional in CSCs. We first used electron microscopy to

examine thin sections of GBM xenografts and CSC spheres grown in vitro and found structures characteristic of gap junctions, i.e., the plasma membranes of two adjacent cells were in close proximity but separated by a narrow gap (Figure 1A). To confirm whether functional cell-cell communication occurred among CSCs, we microinjected a fluorescent dye into single CSCs in monolayer cultures and assessed cell-cell communication by tracking diffusion of the injected dye. To achieve this, we took advantage of a co-injection strategy in which the parental cell was injected with a fluorescent IgG too large to be transferred to adjacent cells (<150 kDa) in combination with fluorescent dyes small enough to diffuse between adjacent cells through gap junctions (<1 kDa, Figure 1B). Overtime, the dye rapidly diffused to adjacent cells as observed by time-lapse imaging (Figure 1C). Using this approach with multiple fluorescent dyes (lucifer yellow and the glucose analog 2NBGD), we observed direct cell-cell communication between CSCs as well as between non-CSCs and between CSCs and non-CSCs in a bidirectional manner (data not shown).

To confirm that this diffusion was mediated by gap junctions, we utilized several compounds with gap junction inhibitory properties: carbenoxolone (CBX), 1-heptanol, mefloquine (MEF), and 1-octanol (Juszczak and Swiergiel, 2009; Rozental et al., 2001). CBX is approved for use in the United Kingdom for inflammation and gastriculcers, MEF is an anti-malarialagent, 1-heptanol and 1-octanol are approved for use in the United States and found as additives in perfume, and 1-octanol also currently is being evaluated for efficacy against essential trem or (Nahab et al., 2011). We repeated the single-cell injection studies in the presence of either CBX or 1-octanol and observed a significant reduction in dye diffusion in CSCs (Figure 2) and non-CSCs (data not shown). We further confirmed the efficacy of all four inhibitors using a flow cytometry-based assay, and each inhibitor significantly attenuated dye diffusion in CSCs derived from multiple xenograft specimens (data not shown). These data confirm the presence of functional gap junctions between CSCs.

Gap Junction Inhibitors Are Toxic to CSCs and Inhibit CSC Proliferation and Self-Renewal

Based on our observations of functional gap junctions between CSCs, we wanted to determine whether gap junction inhibitors could be used to target CSCs. We tested the impact of CBX (100 mM) and 1-octanol (1 mM) on the growth of CSCs and non-CSCs. In CSCs derived from multiple xenografts, we observed a significant reduction in CSC growth. The inhibitory effect on CSCs was greater than what was observed in non-CSCs in optimized media for each cell type (Figure 3A). However, when identical media conditions were used, the growth of both CSCs and non-CSCs was impacted (Figure S1A). To determine whether these gap junction inhibitors attenuated self-renewal, we performed in vitro limiting dilution studies across a range of CBX and 1-octanol concentrations, and we found that gap junction inhibitors reduced sphere formation and stem cell frequency (Figures 3B and 3C).

To determine the mechanism by which gap junction inhibitors reduced proliferation and self-renewal, we evaluated apoptotic events using a caspase-3/7 activity assay and found a significant increase in caspase-3/7 activity when CSCs were exposed to gap junction inhibitors (Figure S1B). To address whether the inhibitory effect of CBX and 1-octanol was

CSC specific, we compared the IC_{50} for CSCs and NPCs and found that both inhibitors had a significantly lower IC_{50} in CSCs compared to NPCs (36.5 versus 49.5 mM for CBX and 2.1 versus 2.4 mM for 1-octanol, $p < 0.01$, sigmoidal dose response/comparison off its, data not shown). We then tested cell viability across CSCs from multiple GBM xenografts after a 3-day treatment with the compounds at the IC_{50} values and found a significant reduction in viability compared with NPCs (Figure S1C). No difference in viability was observed with 4-methyl-heptanol, an isomer of 1-octanol lacking gap junction inhibitory activity (Figure S1C). These data demonstrate that multiple gap junction inhibitors can target CSC proliferation and self-renewal.

Gap Junction Inhibitors Attenuate Tumor Growth In Vivo and Greatly Increase Tumor Latency in Combination with Temozolomide

Based on our in vitro data, we investigated the efficacy of gap junction inhibitors on tumor growth in vivo. Using a subcutaneous xenograft model, we evaluated the effect of gap junction inhibitors on tumor growth. After detection of palpable subcutaneous tumors, the mice were randomized and treated with a gap junction inhibitor (CBX or 1-octanol), temozolomide (TMZ), or a combination of a gap junction inhibitor and TMZ, and tumor volume was monitored over time. Tumor growth was significantly delayed by treatment with either a gap junction inhibitor or TMZ, the standard chemotherapeutic treatment for GBM (Figure 3D). An additive effect on tumor growth suppression was observed when a gap junction inhibitor and TMZ were combined (Figure 3D). We also used an orthotopic xenograft model to assess the anti-tumor effect of 1-octanolalone and in combination with TMZ. Treatment of an established intracranial tumor with CBX or 1-octanol initiated 14 days after tumor cell inoculation increased tumor latency and median survival compared with control treatments, indicating a strong correlation between gap junction inhibitory activity and anti-tumor effect (Figure 3E). Based on the ability of 1-octanol to significantly increase tumor latency, we combined 1-octanol with the chemotherapeutic TMZ. The 1-octanol treatment enhanced the effect of TMZ, as the combination treatment robustly increased the survival of mice (Figure 3E), decreased proliferation, and induced apoptosis (data not shown).

As gap junction inhibitors augmented the anti-tumor effect of TMZ in both subcutaneous and orthotopic xenograft models, we next interrogated whether gap junction inhibitors sensitized TMZ-resistant GBM cells to TMZ. Using an in vitro model, we compared the growth of TMZ-resistant GBM cells treated with TMZ alone with those treated with TMZ and CBX in combination. This combined treatment significantly inhibited the growth of the resistant tumor cells and decreased the rate of symmetric cell division (Figures S1D and S1E). Taken together, these data demonstrate the anti-tumor effect of gap junction inhibition in pre-clinical GBM models and suggest increased efficacy when combined with TMZ. In addition, these data indicate that the growth of TMZ-resistant cells can be attenuated by gap junction inhibition, which correlated with a sensitization of TMZ-resistant cells to TMZ.

Connexin Subunit Expression Analysis Demonstrates that Cx46 Is Enriched in CSCs

Based on our identification of functional gap junctions in CSCs and the efficacy of gap junction inhibitors on attenuating CSC maintenance, we wanted to determine which

connexins were responsible for these effects. We evaluated the expression of different connexins in NPCs and well-established human GBM - derived xenograft tumors (T4121 and T387), consisting of populations of CSCs and non-CSCs with functionally high (CSC) or low (non-CSC) tumor initiation capabilities. We performed qPCR and found that Cx46 was significantly elevated in CSCs compared with NPCs and that Cx43 was elevated in NPCs compared with CSCs (Figure S2A). Cx46 has not been well described in many tissues outside of the eye (Gong et al., 1997), w here it has been linked to congenital cataract formation (Mackay et al., 1999). It also has been reported that Cx46 is reciprocally regulated with Cx43 (Banerjee et al., 2011) and may be responsive to hypoxia (Molina and Takemoto, 2012), a microenvironmental CSC maintenance factor (Li et al., 2009; Soeda et al., 2009).

To evaluate differences between CSCs and non-CSCs, we performed immunoblotting analysis with an antibody validated by detection of the product of a cDNA encoding human Cx46 and the absence of Cx46 in Cx46 knockout mouse lens tissue. This antibody revealed that Cx46 was enriched in CD133+ CSCs compared with matched CD133+ non-CSCs from the same tumor (Figure 4A). Cx43 was expressed at much lower levels in CSCs than in non-CSCs (Figure 4A). To determine whether this differential Cx43 expression was regulated epigenetically, we analyzed publically available chromatin immunoprecipitation followed by sequencing (ChIP-seq) datasets containing H3K27ac information of three primary GBM samples cultured under stem cell growth conditions (TPC) or differentiation conditions (DGC) (Figure S2B; Suvà et al., 2014). We found striking activation of promoter and enhancer elements surrounding the Cx43 gene locus in the differentiated glioma cells, suggesting that the differences we observed in Cx43 protein and RNA levels were governed epigenetically through histone modifications. The elevated expression ofCx46 in CSCs also was detected when CSCs were enriched directly from xenografts based on CD133 oran alternative CSC marker, integrin α6 (Lathia et al., 2010; Figure 4B; Figure S2C). Our expression analysis revealed that Cx46 was expressed by CSCs, while Cx43 was expressed by non-CSCs. As CSCs differentiate, the expression of molecules involved in CSC maintenance is lost, and the expression of differentiation-associated molecules increases. To evaluate whether Cx46 and Cx43 are located on different ends of the differentiation spectrum, we differentiated CSCs by removing growth factors and adding 10% serum and observed a concomitant decrease in Cx46 along with an increase in Cx43 expression (Figure 4C). Taken together, these data demonstrate that Cx46 is enriched in CSCs and that Cx43 is expressed in non-CSCs and increases upon CSC differentiation.

Cx46 Is Essential for CSC Proliferation, Self-Renewal, and Tumor Initiation

To interrogate the biological role of Cx46 in CSC maintenance, we generated non-overlapping small hairpin RNA (shRNA) constructs against the Cx46 mRNA (Figure S2D). We confirmed that these constructs reduced Cx46 expression in CSCs (Figure 4D; Figure S2E). After transducing these shRNA constructs into CSCs via lentivirus, we compared cellular functions of transduced CSCs with those receiving a non-targeting control shRNA (NT). Reduced Cx46 expression resulted in decreased proliferation (Figure 4E) and self-renewal (Figures 4F and 4G), as well as reduced stem cell frequency (Figure 4G). In addition, the decreases in proliferation and self-renewal were accompanied by an increase in cell death as assessed by caspase-3/7 activity (Figure S2F). To determine whether Cx46 was

essential for tumor initiation, an in vivo surrogate assay of CSC self-renewal, we transduced CSCs with NT or Cx46 shRNA constructs and evaluated their tumor formation ability by transplanting the cells into the brains of immunocompromised mice. Across multiple cell dosages (1,000 and 10,000 cells), CSCs containing the NT construct uniformly formed tumors, whereas CSCs transduced with Cx46-targeting shRNAs demonstrated significantly increased tumor latency and a reduced tumor formation capacity (Figure 4H). Taken together, these data demonstrate that Cx46 is essential for CSC maintenance.

CSCs Predominantly Express Cx46, and Non-CSCs Express Cx43, Resulting in Different Diffusion Rates and Resting Membrane Potential

To determine the physiological consequence of differential connexin subunit expression by CSCs and non-CSCs, we evaluated dye diffusion rates between cells and resting membrane potential, as Cx46 and Cx43 have different diffusion rates and ion selectivity (Elfgang et al., 1995; Lin et al., 2004). Cx43 allows for the passage of both cations and anions, whereas Cx46 only allows for the passage of cations (Harris, 2001; Qu and Dahl, 2002; Trexler et al., 2000; Wang and Veenstra, 1997). Using a dye-diffusion-based assay to measure de novo gap junction formation (Figure 5A), we evaluated the time until dye diffusion was established between CSCs and between non-CSCs as an indicator of the gap-junction-forming capacity of these cells. We observed that the establishment of new gap junctions was significantly faster in CSCs compared with non-CSCs (Figure 5B). Depletion of Cx46 from CSCs by shRNA resulted in decreased dye diffusion (Figure 5C), suggesting that new gap junctions formed more slowly and demonstrating the role of Cx46 in this process.

We voltage-clamped CSCs and non-CSC and observed a decreased outward current in CSCs (Figure 5D) and significantly depolarized resting membrane potential (Figure 5E), which may be due to a decrease in cell membrane ionic permeability for potassium ions. Whole-cell voltage clamp analysis revealed reduced potassium current density in CSCs compared with non-CSCs (data not shown). Based on differences in connexin expression between CSCs and non-CSCs as well as the rate of cell-cell communication and resting membrane potential, we set out to determine whether the expressions of Cx46 and Cx43 were linked as reported in the lens (Banerjee et al., 2011). To evaluate whether Cx43 suppressed Cx46 expression in GBM cells, we generated non-overlapping shRNA constructs against the Cx43 mRNA (Figure S2B) and found that a reduction in Cx43 in non-CSCs resulted in an increase in Cx46 (Figure 5F). Non-CSCs depleted of Cx43 possessed an increased membrane potential, with the values for some cells falling within the range of values observed for CSCs (Figure 5G), and this result was consistent with the increased level of Cx46 in these cells. Taken together, these data suggest that the differential expression of connexin subunits between CSCs and non-CSCs is in part linked to the differentiation process and that these changes in connexin subunits affect de novo gap junction formation and resting membrane potential.

Cx46, but Not Cx43, Expression Predicts GBM Patient Survival

Based on our observations of the roles of gap junctions and individual connexin subunits in GBM cells, we sought to determine whether expression differences correlated with GBM patient prognosis. We first analyzed bioinformatics data to determine whether changes in the

molecules expressed at cell-cell interfaces, including connexins, predicted GBM patient prognosis by interrogating the tight junction interaction gene set in Oncomine, which contains 26 genes expressed at cell junctions including some connexin subunits (Figure S3A). As a whole, elevated levels in this gene set significantly correlated with poor glioma patient prognosis (Figure S3B) and included proteins that previously have been reported in GBM progression, such as epidermal growth factor receptor (EGFR)(Mazzoleni et al., 2010) and junctional adhesion molecule-A (JAM-A), which we recently reported to be elevated in CSCs (Lathia et al., 2014).

We interrogated the correlation between expression levels of individual genes and GBM patient survival across multiple other datasets in both Oncomine and the National Cancer Institute (NCI) Repository for Molecular Brain Neoplasia Data (REM BRANDT) and found that Cx46 elevation consistently correlated with poor prognosis of glioma and GBM patients (Figure 6A; Figure S3C). Cx46 also negatively correlated with patient survival in the classical molecular subtype in The Cancer Genome Atlas (TCGA) dataset, but did not correlate with survival in the mesenchymal or proneural subtypes (Figure 6B, data not shown). Cx43 showed no consistent correlation with patient survival (Figures 6C and 6D; Figure S3C), nor did other connexin subunits in the dataset (Cx31, Cx43, Cx45, and Cx50; data not shown). Taken together, our bioinformatics analysis revealed that proteins expressed at intercellular junctions inform GBM patient survival and demonstrated that Cx46 levels correlate with poor GBM patient prognosis, which support our findings that Cx46 is essential for CSC maintenance.

DISCUSSION

Gap junctions have been show n to play a tumor-suppressive role (Kandouz and Batist, 2010); however, our data indicate that the connexin composition of gap junctions dictates their function, which can be tumorigenic. Gap-junction-mediated communication plays critical roles in coordinating m any cellular processes, such as electrophysiological activity, proliferation, cell survival, and differentiation to maintain tissue homeostatic integrity (Wei et al., 2004; White and Paul, 1999). Therefore, reduced expression of connexins has been considered a mechanism that enables tumor cells to escape from the instructions of the tissue and obtain malignant phenotypes, such as continued proliferation, uncontrolled migration, and invasion. Reduced connexin levels have been reported in GBM, and restoring expression inhibited tumor growth (Hao et al., 2012; Huang et al., 2002; Soroceanu et al., 2001; Yu et al., 2012). However, our study uncovers a pro-tumorigenic role for Cx46 that is essential for CSC maintenance. Similar roles for gap junctions have been experimentally demonstrated in somatic stem cells during regeneration (Foss et al., 2009; Jäderstad et al., 2010), in the germ line (Tazuke et al., 2002), and in embryonic stem cells (Todorova et al., 2008; Wong and Pébay, 2010). Based on the pro- and anti-tumor effects of connexins, a comprehensive investigation of gap junctions that takes into account connexin diversity will be required to understand the role of gap junctions during tumor growth.

Our observation that Cx46 and Cx43 exist on different ends of the differentiation spectrum of GBM cells supports diverse roles for connexins and suggests that connexin specificity may be essential for transitions between self-renewal and differentiation. Our data also

confirm previous findings in the lens by showing that Cx43 reduction in non-CSCs increases Cx46 expression. However, unlike the reciprocal relationship between Cx46 and Cx43 in the lens (Banerjee et al., 2011), knockdown of Cx46 in CSCs did not increase Cx43 expression, or self-renewal, or resting membrane potential, nor did overexpression of Cx46 in non-CSCs decrease Cx43 expression (data not shown), suggesting that there are additional regulatory elements between Cx46 and Cx43. These observations raise a fundamental question: why do different cells require different connexins? Several possibilities exist including the physical properties of cell-cell communication (speed of communication and ion selectivity) that may result in differences in membrane potential depolarization serving as an electrical signal to activate voltage-dependent plasma membrane proteins. This hypothesis is supported by our observation that CSCs exhibit elevated dye diffusion, a surrogate for increased gap junction coupling, and have a reduced resting membrane potential. The differences in resting membrane potential also may reflect an indirect regulation of ion diffusion, which would be a useful area for future inquiry.

Interestingly, we observed a correlation between high Cx46 expression and poor patient prognosis in the classical subtype, but not in the proneural or mesenchymal subtypes, of GBM. The difference in the proneural molecular subtype where Cx43 was more negatively correlated with patient prognosis may be related to observations of inhibition of gap-junction-mediated intercellular communication by platelet-derived growth factor (PDGF) signaling (Yao et al., 2000), a hall mark mutation in the subtype; thus, a decreased reliance on gap junction communication mediated by PDG F receptor signaling in the proneural subtype may reduce the selective pressure to express specific connexin isoforms. Additional connexin-specific evaluations will be required to fully elucidate the contribution of connexin subunits to self-renewal and modulation of physical properties. In addition, future studies also need to consider the growing evidence that connexin function may be controlled by cytoplasmic tail interactions (Dbouk et al., 2009), the interaction between individual connexin subunits and scaffolding proteins or cadherins, such as the recently demonstrated interaction between Cx43 and E-cadherin (Yu et al., 2012), which may provide additional opportunities to unravel the complexity of connexin action during tumorigenic processes as well as reveal points of fragility for therapeutic targeting.

Our data also indicate that cell-cell communication is critical for tumor growth and highlight the complexity of anti-tumor approaches through connexin targeting that have mainly focused on increasing connexin expression and gap junction function. Reduced connexin expression in tumors supports a therapeutic approach in which increasing gap junctions would elicit a therapeutic benefit and would be expected to maximize the by stander effect to increase therapeutic efficacy against tumor cells (Cottin et al., 2011). However, recent work has demonstrated that Cx43 is linked to TMZ resistance, which can be reversed by reducing Cx43 expression (Gielen et al., 2013; Munoz et al., 2014), thereby supporting a therapeutic approach based on reducing connexin levels. Our data indicate that targeting gap junction function using inhibitors, such as 1-octanol and CBX, is associated with attenuated CSC maintenance and tumor progression. While these results must be interpreted in the context of these inhibitors targeting multiple connexin subunits, our genetic approach specifically targeting Cx46, which is enriched in CSCs, revealed an essential role of this connexin subunit in CSC maintenance and GBM growth. The gap junction inhibitors tested

in this study are approved for clinical use, and 1-octanolis currently under investigation for essential trem or (Nahab et al., 2011; Shill et al., 2004). The activity of these inhibitors against GBM encourages the clinical application of these agents to treat GBM, a disease that responds poorly to current therapeutics.

To pursue this direction, determining the effective and tolerable concentrations of gap junction inhibitors is an important next step, because gap junctions function ubiquitously in many organs and tissues to regulate physiological functions. Hence, it would be desirable to develop inhibitors with specificity for the connexin isotype essential for CSCs, such as Cx46, although the anti-tumor dosages of general gap junction inhibitors were tolerated in our current in vivo animal models. In addition to their own anti-GBM effects, these gap junction inhibitors enhanced the anti-tumor effect of TMZ, the standard chemotherapeutic agent used to treat GBM, which also was observed in recent studies on Cx43 (Gielen et al., 2013; Munoz et al., 2014). Furthermore, we demonstrate that gap junction inhibitors can sensitize TMZ-resistant GBM cells. These findings suggest that gap junction inhibitors can be used to override the development of TMZ resistance and potentially that of other chemotherapy drugs as well. Similarly, gap junction inhibition is reported to enhance the cytotoxicity induced by TRAIL stimulation in glioma (Yulyana et al., 2013). The presence of a gap junction network system among tumor cells in GBM, as demonstrated by this study, contributes to CSC maintenance and tumor growth in a connexin-isotype-dependent manner and provides a unique therapeutic opportunity for the development of more effective anti-GBM therapies.

EXPERIMENTAL PROCEDURES

GBM Cell Collection, Culture, and Usage

GBM cells were dissociated from specimens collected from patients, under written consent according to a protocol approved by the Cleveland Clinic and University of Florida Institutional Review Boards, and maintained as subcutaneous xenografts. CSCs and non-CSCs were generated from these xenografts as described in the Supplemental Experimental Procedures.

Proliferation, Sphere Formation, and Tumor Initiation Assays

Cell proliferation, self-renewal, and tumor initiation assays were performed as previously described (Bao et al., 2006; Eyler et al., 2011; Guryanova et al., 2011; Lathia et al., 2010; Li et al., 2009). Relevant experimental details are described in the Supplemental Experimental Procedures.

Electron Microscopy

CSC spheres were collected by centrifugation, and subcutaneous xenograft tumors were obtained by cutting a portion of the tumors into small pieces less than 1 mm^3. The samples were fixed with 10% form aldehyde, 2% paraformaldehyde, 2.5% glutaraldehyde, and 2.5% dimethylsulfoxide in Millonig's phosphate buffer for 2 hr at room temperature. After rinsing, the specimens were post-fixed with 3% potassium ferrocyanide and 2% aqueous osmium tetroxide twice for 1 hr each. Samples were stained with 0.25% uranylacetate,

dehydrated, and embedded into propylene oxide resin. Thin sections were made and observed with transmitted electron microscopes, either an FEI TecnaiG 2 Spirit Bio TWIN or a JEOL 1200EX electron microscope.

Immunofluorescence Analysis

Immunostaining analysis on xenografted GBM specimens (generated by intracranial injection of GBM specimens T4121 and T387) was performed as previously described (Lathia et al., 2010). Relevant experimental details are described in the Supplemental Experimental Procedures.

Gap Junction Dye Diffusion Assay

To quantify gap-junction-mediated intercellular diffusion, we used three separate approaches: (1) analyzing diffusion of calcein from loaded cells by flow cytometry, (2) analyzing calcein diffusion by time-lapse imaging, and (3) performing microinjection-based analysis. The flow cytometric determination was performed similarly as described previously (Fonseca et al., 2006). A single-cell suspension was prepared by trypsinizing a CSC sphere culture the day before the assay. The suspension was separated into two fractions. The donor cells were loaded with calcein AM, and the acceptor cells were labeled with DiD according to the manufacturer's instructions. After the free dye was washed away, both cultures were mixed for various times, stained with DAPI, and fixed with paraformaldehyde. Fluorescence-activated cell sorting (FACS) data were analyzed after gating to eliminate aggregated cells (by forward and side scattering) and dead cells (by DAPI positivity). The percentage of recipient cells that became positive for calcein signal was determined. To analyze the kinetics of dye coupling, we also monitored calcein diffusion using time-lapse microscopy. Calcein AM-loaded, DiD-labeled donor cells in suspension were plated onto monolayer cultures of unlabeled recipient cells. To determine gap junction activity, recorded images were analyzed for the density of calcein dye uptake by unlabeled cells and calcein retained by DiD-labeled donor cells using ImageJ.

To determine gap-junction-dependent dye diffusion, cells were grown on a coverslip coated with Geltrex and cultured in neurobasal media with B27, EGF, and bFGF. A single cell was co-injected with lucifer yellow or 2-deoxy-2-[(7-nitro-2,1,3-benzoxadiazol-4-yl)amino]-D-glucose (2NBDG), a fluorescent glucose analog, together with Cy5-labeled IgG. Immediately after microinjection, time-lapse video microscopy was used to capture phase contrast, green fluorescent(for lucifer yellow or 2 NBDG), and far-red fluorescent (for Cy5 IgG) images. The Cy5 IgG image defines the initially injected donor cells, and the green signal outside of this donor cell is the dye diffused to neighboring cells. The fluorescent signals of the dye retained in the donor cells and the dye exported were quantified after thresholding green and far-red fluorescent images using the W and tool of ImageJ.

qPCR and Immunoblot Analysis

The qPCR and immunoblot analysis was performed as previously described (Bao et al., 2006; Eyler et al., 2011; Guryanova et al., 2011; Lathia et al., 2010; Li et al., 2009). Relevant experimental details are described in the Supplemental Experimental Procedures.

Patch Clamping to Record Membrane Potentials and Inward Current

CSCs and non-CSCs were plated at low density in 35-mm dishes and incubated at 37°C in 10% CO2 for at least 24 hr before recording using the whole-cell configuration of the patch-clamp technique at room temperature (22°C–24°C). Patch pipettes (3.5–4.5 MU) were pulled (P-1000, Sutter Instruments) from micropipette glass (Fisher Scientific) and fire-polished (MF-830, Narashige). Recording pipettes contained the following: KCl (130 mM), EGTA (10 mM), HEPES (10 mM), $CaCl_2$ (1 mM), and $MgCl_2$ (1 mM [pH 7.3]). For CSCs and non-CSCs, the bath solution contained the following: NaCl (136 mM), KCl (4 mM), $MgCl_2$ (2 mM), $CaCl_2$ (1 mM), HEPES (10 mM), and glucose (10 mM [pH 7.4]).

Current-clamp experiments were performed to record the cell's resting membrane potential. All voltage- and current-clamp experiments were performed using an Axopatch 200B amplifier (Molecular Devices) interfaced to a Dell Precision T1600 computer with a Digidata 1440 analog/digital interface and the pCLAM P 10 software package (Molecular Devices). Data were filtered at 5 kHz before storage and offline analysis (Clam pfit10). Voltage protocols were delivered at 10-s intervals. Approximately 80% of series resistance was compensated with the voltage-clamp circuitry. Inward and outward currents were recorded in response to 10-ms voltage steps to test potentials between −120 and +80 mV from a holding potential (HP) of −80 mV.

Bioinformatics Analysis

The Oncomine Platform (Life Technologies) was used for analysis of patient data. Genes used to form the tight junction index were taken from the Human Protein Reference Database (HPRD) interaction set with tight junction protein 1 (TJP1), accessed through Oncomine. Expression levels of these genes were combined to create a tight junction index for each patient with survival data from the available datasets. Survival comparisons are between patients with higher- or lower-than-average gene expression or tight junction index score, visualized via Kaplan-Meier analysis and assessed for significance via log-rank test. Oncomine data were accessed at https://www.oncomine.org. NCIREM BRANDT data were accessed at https://caintegrator.nci.nih.gov/rembrandt/. TCGA data were accessed at https://tcga-data.nci.nih.gov/tcga/tcgaHome2.jsp.

ChIP-Seq Analysis

We obtained published datasets of histone H3K27ac ChIP-seq data (Suvà et al., 2014) and norm albrain regions (ENCODE consortium), and we viewed the aligned data using the Integrative Genomics Viewer (IGV) browser tool (Broad Institute, https://www.broadinstitute.org). Track scales were matched among all paired samples.

Statistical Analysis

Values reported in the results are mean values ± SD, and statistical analysis was performed using Sigma Stat (version 3.5). Unless otherwise stated, one-way ANOVA was used to calculate statistical significance; p values are detailed in the text and figure legends. In vivo survival analysis was calculated by log-rank analysis.

Supplementary Material

Refer to Web version on PubMed Central for supplementary material.

ACKNOWLEDGMENTS

We thank the members of the J.D.L. and B.A.R. laboratories for constructive comments on the experimental design and manuscript. We thank Cathy Shemo, Patrick Barrett, and Sage O'Bryant for flow cytometry assistance; the Cleveland Clinic Foundation Tissue Procurement Service; Dr. Susan Staugaitis; Dr. Robert Weil; and Mary McGraw. We also thank Noah Bar-Shain, Vid Yogeswaran, Dr. Midori Hitomi, and Dr. Hisashi Fujioka at the Case Western Reserve University electron microscopy facility for excellent technical assistance. We thank Dr. Mahendra S. Rao (New York Stem Cell Foundation) for providing NPCs. These studies were supported by grant IRG-91-022-18 to the Case Comprehensive Cancer Center from the American Cancer Society to J.D.L. Work in the J.D.L. lab also is supported by NIH grants CA157948, NS083629, and CA191263; the Sontag Foundation; the Lerner Research Institute; Blast GBM; a VeloSano Pilot Research Award; Voices Against Brain Cancer; the Ohio Cancer Research Associates; and a V Scholar Award from the V Foundation for Cancer Research. Work in the B.A.R. lab is supported by NIH grant CA141020, the National Brain Tum or Society, Florida Center for Brain Tumor Research, and an IFAS Research Innovation Grant. Work in the J.N.R. lab is supported by NIH grants CA112958, CA154130, CA169117, NS087913, and NS089272.

REFERENCES

Banerjee D, Das S, Molina SA, Madgwick D, Katz MR, Jena S, Bossmann LK, Pal D, Takemoto DJ. Investigation of the reciprocal relationship between the expression of two gap junction connexin proteins, connexin46 and connexin43. J. Biol. Chem. 2011; 286:24519–24533. [PubMed: 21606502]

Bao S, Wu Q, Mc Lendon RE, Hao Y, Shi Q, Hjelmeland AB, Dewhirst MW, Bigner DD, Rich JN. Glioma stem cells promote radio resistance by preferential activation of the DNA damage response. Nature. 2006; 444:756–760. [PubMed: 17051156]

Beyer EC, Berthoud VM. Connexin hemichannels in the lens. Front. Physiol. 2014; 5:20. [PubMed: 24575044]

Cheng A, Tang H, Cai J, Zhu M, Zhang X, Rao M, Mattson MP. Gap junctional communication is required to maintain mouse cortical neural progenitor cells in a proliferative state. Dev. Biol. 2004; 272:203–216. [PubMed: 15242801]

Cottin S, Gould PV, Cantin L, Caruso M. Gap junctions in human glioblastom as: implications for suicide gene therapy. Cancer Gene Ther. 2011; 18:674–681. [PubMed: 21779029]

Dbouk HA, Mroue RM, El-Sabban ME, Talhouk RS. Connexins: a myriad of functions extending beyond assembly of gap junction channels. Cell Commun. Signal. 2009; 7:4. [PubMed: 19284610]

Elfgang C, Eckert R, Lichtenberg-Frate H, Butterweck A, Traub O, Klein RA, Hülser DF, Willecke K. Specific permeability and selective formation of gap junction channels in connexin-transfected He La cells. J. Cell Biol. 1995; 129:805–817. [PubMed: 7537274]

Elias LA, Wang DD, Kriegstein AR. Gap junction adhesion is necessary for radial migration in the neocortex. Nature. 2007; 448:901–907. [PubMed: 17713529]

Evans WH, Martin PE. Gap junctions: structure and function (Review). Mol. Membr. Biol. 2002; 19:121–136. [PubMed: 12126230]

Eyler CE, Wu Q, Yan K, Mac Swords JM, Chandler-Militello D, Misuraca KL, Lathia JD, Forrester MT, Lee J, Stamler JS, et al. Glioma stem cell proliferation and tumor growth are promoted by nitric oxide synthase-2. Cell. 2011; 146:53–66. [PubMed: 21729780]

Fonseca PC, Nihei OK, Savino W, Spray DC, Alves LA. Flow cytometry analysis of gap junction-mediated cell-cell communication: advantages and pitfalls. Cytometry A. 2006; 69:487–493. [PubMed: 16646046]

Foss B, Hervig T, Bruserud O. Connexins are active participants of hematopoietic stem cell regulation. Stem Cells Dev. 2009; 18:807–812. [PubMed: 19355839]

Galli R, Binda E, Orfanelli U, Cipelletti B, Gritti A, De Vitis S, Fiocco R, Foroni C, Dimeco F, Vescovi A. Isolation and characterization of tumorigenic, stem-like neural precursors from human glioblastoma. Cancer Res. 2004; 64:7011–7021. [PubMed: 15466194]

Gerido DA, De Rosa AM, Richard G, White TW. Aberrant hemichannel properties of Cx26 mutations causing skin disease and deafness. Am. J. Physiol. Cell Physiol. 2007; 293:C337–C345. [PubMed: 17428836]

Gielen PR, Aftab Q, Ma N, Chen VC, Hong X, Lozinsky S, Naus CC, Sin WC. Connexin43 confers Temozolomide resistance in human glioma cells by modulating the mitochondrial apoptosis pathway. Neuropharmacology. 2013; 75:539–548. [PubMed: 23688923]

Gong X, Li E, Klier G, Huang Q, Wu Y, Lei H, Kumar NM, Horwitz J, Gilula NB. Disruption of alpha 3 connexin gene leads to proteolysis and cataracto genesis in mice. Cell. 1997; 91:833–843. [PubMed: 9413992]

Guryanova OA, Wu Q, Cheng L, Lathia JD, Huang Z, Yang J, Mac Swords J, Eyler CE, Mc Lendon RE, Heddleston JM. Nonreceptor tyrosine kinase BMX maintains self-renewal and tumorigenic potential of glioblastoma stem cells by activating STAT3. Cancer Cell. 2011; 19:498–511. [PubMed: 21481791]

Hao J, Zhang C, Zhang A, Wang K, Jia Z, Wang G, Han L, Kang C, Pu P. miR-221/222 is the regulator of Cx43 expression in human glioblastoma cells. Oncol. Rep. 2012; 27:1504–1510. [PubMed: 22294051]

Harris AL. Emerging issues of connexin channels: biophysics fills the gap. Q. Rev. Biophys. 2001; 34:325–472. [PubMed: 11838236]

Huang R, Lin Y, Wang CC, Gano J, Lin B, Shi Q, Boynton A, Burke J, Huang RP. Connexin43 suppresses human glioblastoma cell growth by down-regulation of monocytechemotactic protein 1, as discovered using protein array technology. Cancer Res. 2002; 62:2806–2812. [PubMed: 12019157]

Ignatova TN, Kukekov VG, Laywell ED, Suslov ON, Vrionis FD, Steindler DA. Human cortical glial tumors contain neural stem-like cells expressing astroglial and neuronal markers in vitro. Glia. 2002; 39:193–206. [PubMed: 12203386]

Jäderstad J, Jäderstad LM, Li J, Chintawar S, Salto C, Pandolfo M, Ourednik V, Teng YD, Sidman RL, Arenas E, et al. Communication via gap junctions underlies early functional and beneficial interactions between grafted neural stem cells and the host. Proc. Natl. Acad. Sci. USA. 2010; 107:5184–5189. [PubMed: 20147621]

Juszczak GR, Swiergiel AH. Properties of gap junction blockers and their behavioural, cognitive and electrophysiological effects: animal and human studies. Prog. Neuropsychopharmacol. Biol. Psychiatry. 2009; 33:181–198. [PubMed: 19162118]

Kandouz M, Batist G. Gap junctions and connexins as therapeutic targets in cancer. Expert Opin. Ther. Targets. 2010; 14:681–692. [PubMed: 20446866]

Lathia JD, Gallagher J, Heddleston JM, Wang J, Eyler CE, Macswords J, Wu Q, Vasanji A, Mc Lendon RE, Hjelmeland AB, Rich JN. Integrin alpha 6 regulates glioblastoma stem cells. Cell Stem Cell. 2010; 6:421–432. [PubMed: 20452317]

Lathia JD, Li M, Sinyuk M, Alvarado AG, Flavahan WA, Stoltz K, Rosager AM, Hale J, Hitomi M, Gallagher J, et al. High-throughput flow cytometry screening reveals a role for junctional adhesion molecule a as a cancer stem cell maintenance factor. Cell Rep. 2014; 6:117–129. [PubMed: 24373972]

Li Z, Bao S, Wu Q, Wang H, Eyler C, Sathornsumetee S, Shi Q, Cao Y, Lathia J, Mc Lendon RE, et al. Hypoxia-inducible factors regulate tumorigenic capacity of glioma stem cells. Cancer Cell. 2009; 15:501–513. [PubMed: 19477429]

Lin GC, Rurangirwa JK, Koval M, Steinberg TH. Gap junctional communication modulates agonist-induced calcium oscillations in transfected He La cells. J. Cell Sci. 2004; 117:881–887. [PubMed: 14762115]

Liu G, Yuan X, Zeng Z, Tunici P, Ng H, Abdulkadir IR, Lu L, Irvin D, Black KL, Yu JS. Analysis of gene expression and chemoresistance of CD133+ cancer stem cells in glioblastoma. Mol. Cancer. 2006; 5:67. [PubMed: 17140455]

Mackay D, Ionides A, Kibar Z, Rouleau G, Berry V, Moore A, Shiels A, Bhattacharya S. Connexin46 mutations in autosomal dominant congenital cataract. Am. J. Hum. Genet. 1999; 64:1357–1364. [PubMed: 10205266]

Mazzoleni S, Politi LS, Pala M, Cominelli M, Franzin A, Sergi Sergi L, Falini A, De Palma M, Bulfone A, Poliani PL, Galli R. Epidermal growth factor receptor expression identifies functionally and molecularly distinct tumor-initiating cells in human glioblastoma multiforme and is required for gliomagenesis. Cancer Res. 2010; 70:7500–7513. [PubMed: 20858720]

Molina SA, Takemoto DJ. The role of Connexin46 promoterin lens and other hypoxic tissues. Commun. Integr. Biol. 2012; 5:114–117. [PubMed: 22808311]

Munoz JL, Rodriguez-Cruz V, Greco SJ, Ramkissoon SH, Ligon KL, Rameshwar P. Temozolomide resistance in glioblastoma cells occurs partly through epidermal growth factor receptor-mediated induction of connexin43. Cell Death Dis. 2014; 5:e1145. [PubMed: 24675463]

Nahab FB, Wittevrongel L, Ippolito D, Toro C, Grimes GJ, Starling J, Potti G, Haubenberger D, Bowen D, Buchwald P, et al. An open-label, single-dose, crossover study of the pharmacokinetics and metabolism of two oral for mulations of 1-octanolin patients with essential tremor. Neurotherapeutics. 2011; 8:753–762. [PubMed: 21594724]

Naus CC, Laird DW. Implications and challenges of connexin connections to cancer. Nat. Rev. Cancer. 2010; 10:435–441. [PubMed: 20495577]

Qu Y, Dahl G. Function of the voltage gate of gap junction channels: selective exclusion of molecules. Proc. Natl. Acad. Sci. USA. 2002; 99:697–702. [PubMed: 11805325]

Rozental R, Srinivas M, Spray DC. How to close a gap junction channel. Efficacies and potencies of uncoupling agents. Methods Mol. Biol. 2001; 154:447–476. [PubMed: 11218664]

Scherer SS, Kleopa KA. X-linked Charcot-M arie-Tooth disease. J. Peripher. Nerv. Syst. 2012; 17(Suppl 3):9–13. [PubMed: 23279425]

Shill HA, Bushara KO, Mari Z, Reich M, Hallett M. Open-label dose-escalation study of or al1-octanol in patients with essential tremor. Neurology. 2004; 62:2320–2322. [PubMed: 15210907]

Singh SK, Clarke ID, Terasaki M, Bonn VE, Hawkins C, Squire J, Dirks PB. Identification of a cancer stem cell in human brain tumors. Cancer Res. 2003; 63:5821–5828. [PubMed: 14522905]

Singh SK, Hawkins C, Clarke ID, Squire JA, Bayani J, Hide T, Henkelman RM, Cusimano MD, Dirks PB. Identification of human brain tumour initiating cells. Nature. 2004; 432:396–401. [PubMed: 15549107]

Soeda A, Park M, Lee D, Mintz A, Androutsellis-Theotokis A, McKay RD, Engh J, Iwama T, Kunisada T, Kassam AB, et al. Hypoxia promotes expansion of the CD133-positive glioma stem cells through activation of HIF-1alpha. Oncogene. 2009; 28:3949–3959. [PubMed: 19718046]

Soroceanu L, Manning TJ Jr, Sontheimer H. Reduced expression of connexin-43 and functional gap junction coupling in human gliomas. Glia. 2001; 33:107–117. [PubMed: 11180508]

Stupp R, Hegi ME, Mason WP, van den Bent MJ, Taphoorn MJ, Janzer RC, Ludwin SK, Allgeier A, Fisher B, Belanger K, et al. European Organisation for Research and Treatment of Cancer Brain Tumour and Radiation Oncology Groups; National Cancer Institute of Canada Clinical Trials Group. Effects of radiotherapy with concomitant and adjuvant temozolomide versus radiotherapy alone on survival in glioblastoma in a randomised phase III study: 5-year analysis of the EORTC-NCIC trial. Lancet Oncol. 2009; 10:459–466. [PubMed: 19269895]

Suvà ML, Rheinbay E, Gillespie SM, Patel AP, Wakimoto H, Rabkin SD, Riggi N, Chi AS, Cahill DP, Nahed BV, et al. Reconstructing and reprogramming the tumor-propagating potential of glioblastom a stem-like cells. Cell. 2014; 157:580–594. [PubMed: 24726434]

Tazuke SI, Schulz C, Gilboa L, Fogarty M, Mahowald AP, Guichet A, Ephrussi A, Wood CG, Lehmann R, Fuller MT. A germ line-specific gap junction protein required for survival of differentiating early germ cells. Development. 2002; 129:2529–2539. [PubMed: 11973283]

Todorova MG, Soria B, Quesada I. Gap junctional intercellular communication is required to maintain embryonic stem cells in a non-differentiated and proliferative state. J. Cell. Physiol. 2008; 214:354–362. [PubMed: 17654515]

Trexler EB, Bukauskas FF, Kronengold J, Bargiello TA, Verselis VK. The first extracellular loop domain is a major determinant of charge selectivity in connexin46 channels. Biophys. J. 2000; 79:3036–3051. [PubMed: 11106610]

Visvader JE, Lindeman GJ. Cancer stem cells: current status and evolving complexities. Cell Stem Cell. 2012; 10:717–728. [PubMed: 22704512]

Wang HZ, Veenstra RD. Monovalention selectivity sequences of the rat connexin43 gap junction channel. J. Gen. Physiol. 1997; 109:491–507. [PubMed: 9101407]

Wei CJ, Xu X, Lo CW. Connexins and cell signaling in development and disease. Annu. Rev. Cell Dev. Biol. 2004; 20:811–838. [PubMed: 15473861]

White TW, Paul DL. Genetic diseases and gene knockouts reveal diverse connexin functions. Annu. Rev. Physiol. 1999; 61:283–310. [PubMed: 10099690]

Wong RC, Pébay A. Study of gap junctions in human embryonic stem cells. Methods Mol. Biol. 2010; 584:211–228. [PubMed: 19907980]

Yao J, Morioka T, Oite T. PDGF regulates gap junction communication and connexin43 phosphorylation by PI3-kinase in mesangial cells. Kidney Int. 2000; 57:1915–1926. [PubMed: 10792610]

Yu SC, Xiao HL, Jiang XF, Wang QL, Li Y, Yang XJ, Ping YF, Duan JJ, Jiang JY, Ye XZ, et al. Connexin43 reverses malignant phenotypes of glioma stem cells by modulating E-cadherin. Stem Cells. 2012; 30:108–120. [PubMed: 22131169]

Yulyana Y, Endaya BB, Ng WH, Guo CM, Hui KM, Lam PY, Ho IA. Carbenoxolone enhances TRAIL-induced apoptosis through the upregulation of death receptor 5 and inhibition of gap junction intercellular communication in human glioma. Stem Cells Dev. 2013; 22:1870–1882. [PubMed: 23428290]

Highlights

- **d** Gap junction targeting potently inhibits GBM growth
- **d** Gap junctions have a pro-tumorigenic role that depends on connexin expression
- **d** CSCs express Cx46, which is required for self-renewal
- **d** Connexin expression dictates intercellular communication and membrane potential

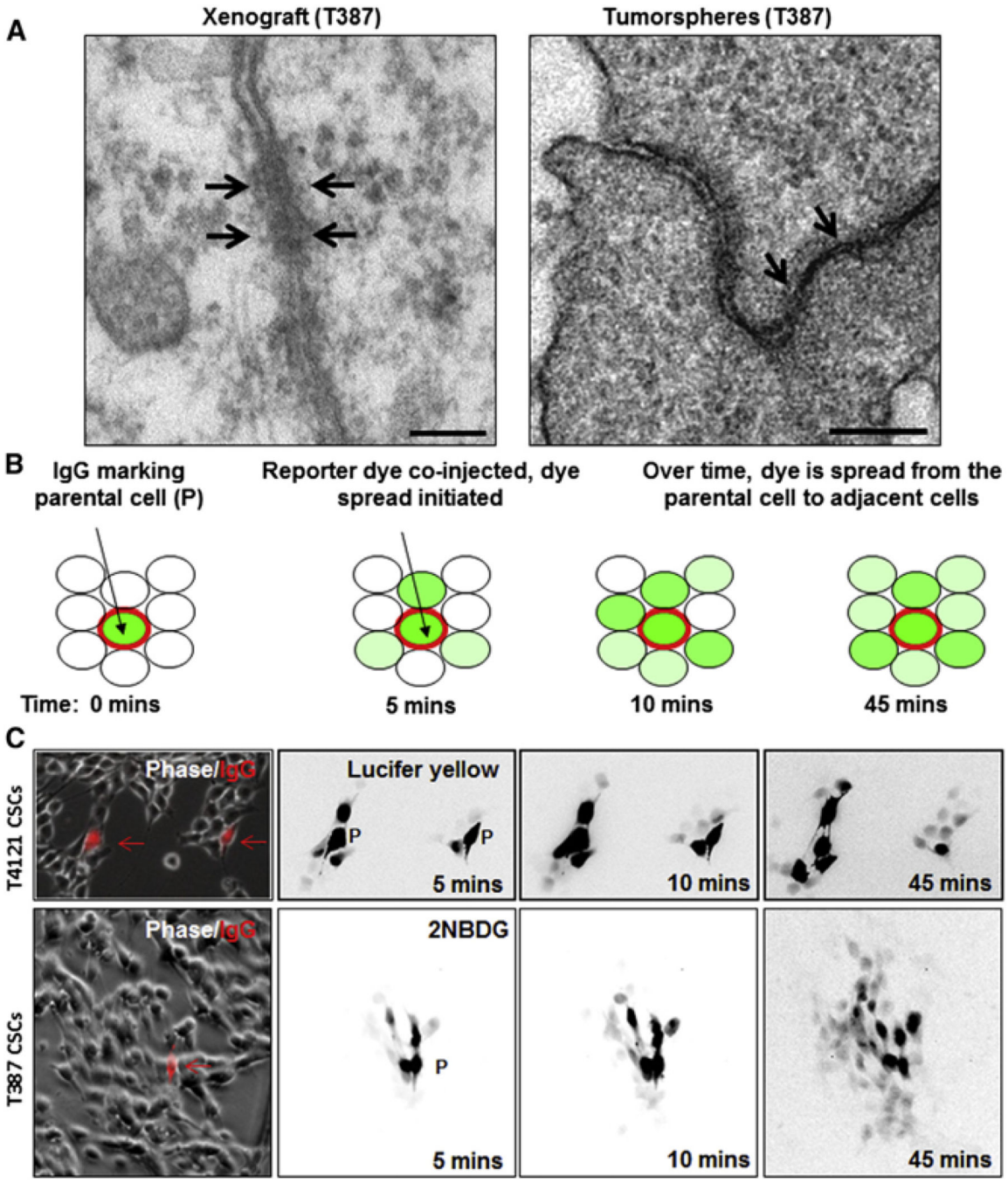

Figure 1. Morphological and Functional Detection of Gap Junctions in CSCs

(A) Electron microscopy evaluation of thin sections from a xenograft tumor and GBM tumorspheres (T387) reveal the presence of gap junction structures. Arrows indicate gap junction structures and scale bar represents 300 nm.

(B) Functional gap junctions in CSCs were evaluated using a microinjection strategy in which the parental cell (P) was injected with a large IgG (red) incapable of leaving the cell and a smaller dye (green), which was visualized spreading to adjacent cells using time-lapse imaging.

(C) Representative micrographs demonstrate the spread of dyes (lucifer yellow and 2NBDG, a fluorescent glucose analog) in CSCs derived from xenografts T4121 and T387.

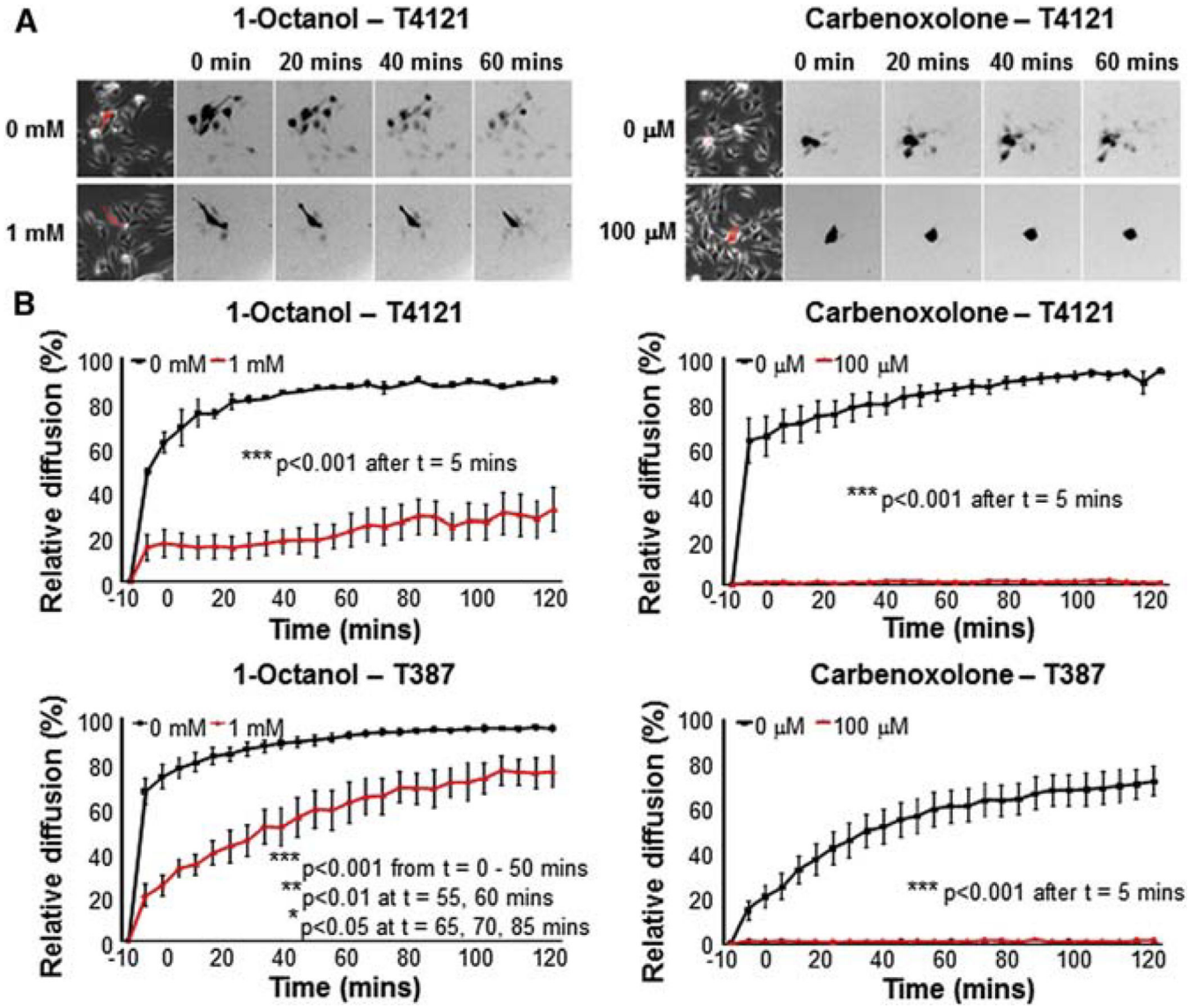

Figure 2. Functional Analysis of Gap Junctions in CSCs

(A and B) Micrographs (A) and quantitative image analysis (B) demonstrate that diffusion of the small molecular-weight fluorescent dye microinjected into CSCs was efficiently blocked by gap junction inhibitors 1-octanol(1 mM) and CBX (100 mM). Data in graphs represent mean values ± SD; *p < 0.05, **p < 0.01 as assessed by one-way ANOVA.

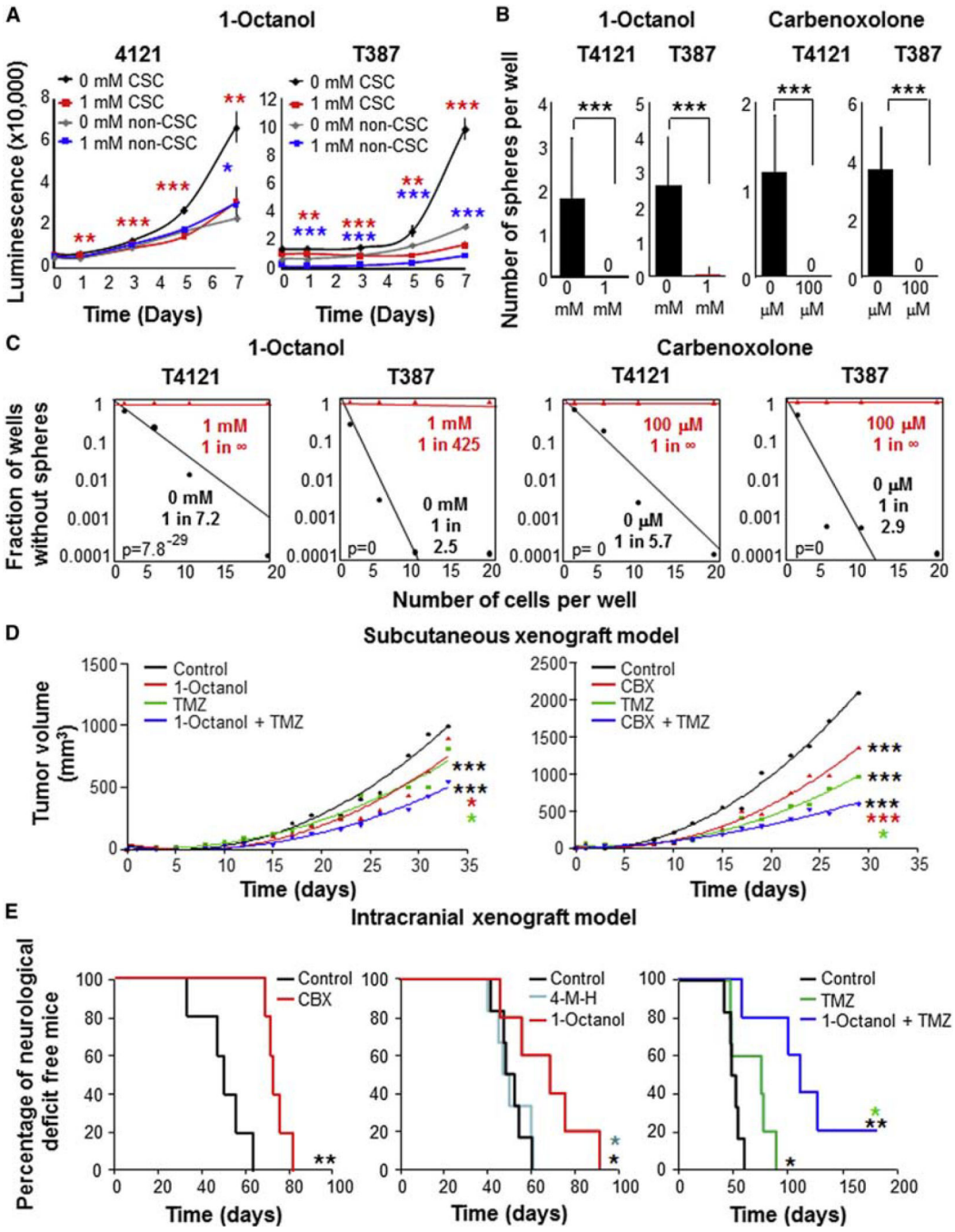

Figure 3. Gap Junction Inhibitors Suppress CSC Proliferation and Self-Renewal

(A) Representative growth curves of CSCs and non-CSCs derived from xenografts T387 and T4121 treated with 1-octanol (1 mM) reveal that CSC growth was significantly attenuated, whereas non-CSC growth was reduced to a lesser degree.

(B and C) Sphere formation from 10 cells per well (B) and limiting dilution analysis (C) reveal that 1-octanol (1 mM) and CBX (100 mM) significantly attenuated CSC self-renewal and reduced stem cell frequency.

(D) Treatment of established subcutaneous tumors with 1-octanol (left) or CBX (right) significantly decreased tumor growth and had an additive effect when combined with TMZ. (E) Treatment of established intracranial tumors with CBX (left) or 1-octanolalone (center) or in combination with TMZ (right) extended survival and increased tumor latency compared with control or a chemical isoform of 1-octanol (4-m ethyl-heptanol) without gap junction inhibitory activity.

Stem cell frequencies are provided directly on each plot; data in graphs represent mean values ± SD;*$p < 0.05$, **$p < 0.01$, ***$p < 0.001$ as assessed by one-way ANOVA. See also Figure S1.

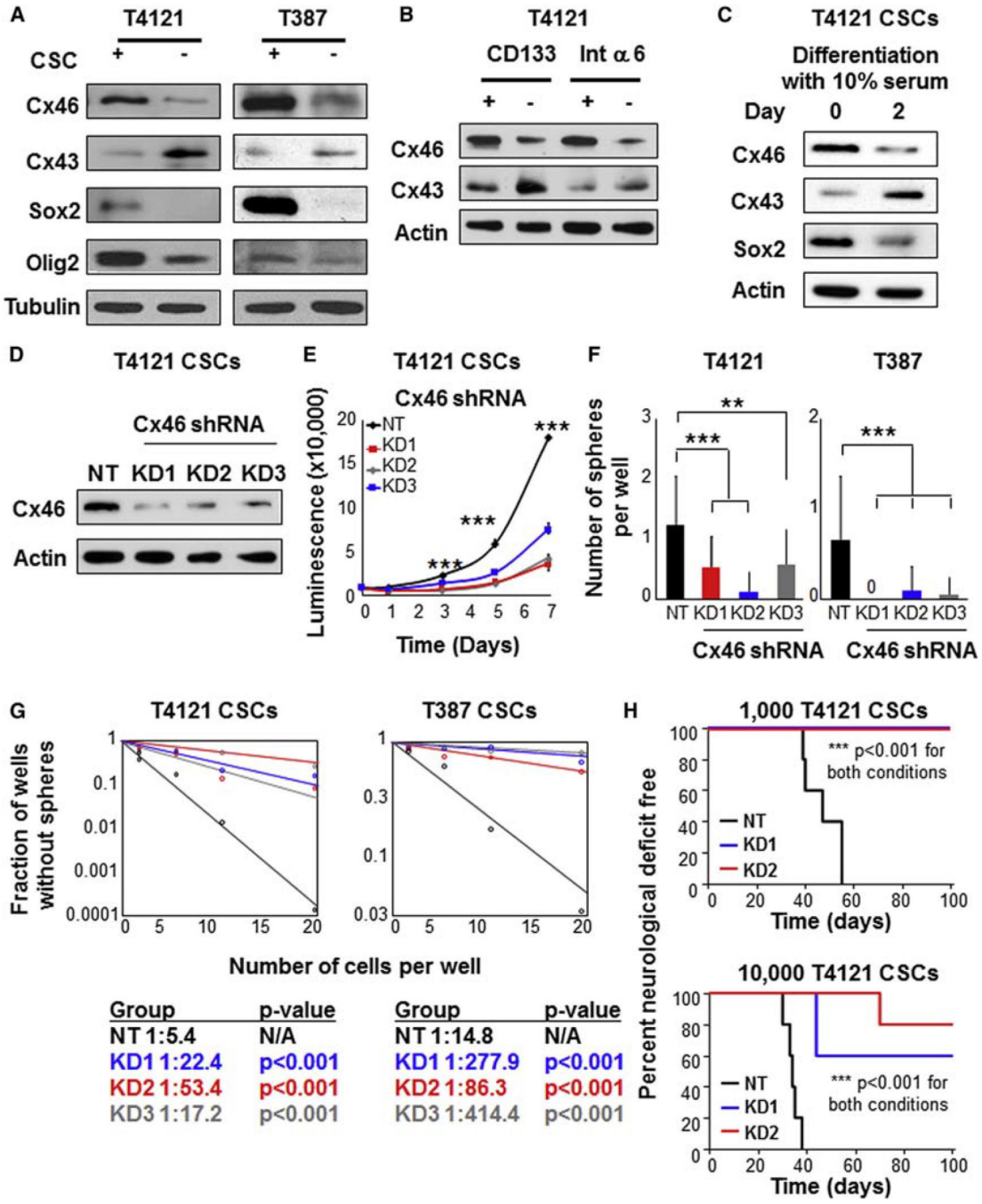

Figure 4. Cx46 Is Enriched in CSCs and Reduction Compromises Proliferation, Self-Renewal, and Tumor Initiation Activity of CSCs

(A) Immunoblotting analysis (A) of CSC and non-CSC populations derived from subcutaneous xenografts (T4121 and T387) reveals that Cx46 expression was elevated in CSCs compared with non-CSC s, whereas Cx43 expression was reduced in CSCs compared with non-CSCs and NPCs.

(B) Immunoblots for Cx46 and Cx43 demonstrate differences in a patient-derived xenograft (T4121) sorted immediately after dissociation for the CSC markers CD133 and integrin α6 (Intα6).

(C) Immunoblotting analysis of CSCs derived from xenograft T4121 reveals that Cx46 expression was reduced during differentiation, whereas Cx43 expression was increased.
(D–G) Cx46 was depleted by lentiviral delivery of shRNA using non-overlapping constructs as demonstrated by representative immunoblots from CSCs derived from xenograft T4121 (D), where Cx46 was reduced by knockdown (KD) constructs compared with the NT control. Cx46 KD suppressed proliferation (E), sphere formation (F), and stem cell frequency (G).
(H) Kaplan-Meier plots of intracranial transplantation of 1,000 (top) or 10,000 (bottom) CSCs with reduced Cx46 expression show decreased tumor formation and increased tumor latency. Tubulin and actin were used as protein loading controls, and a reduction in Sox2 expression was used as a positive control to confirm differentiation.
Data in graphs represent mean values ± SD; *$p < 0.05$, **$p < 0.01$ as assessed by one-way ANOVA and log-rank analysis were used to calculate statistical significance for in vivo studies. See also Figure S2.

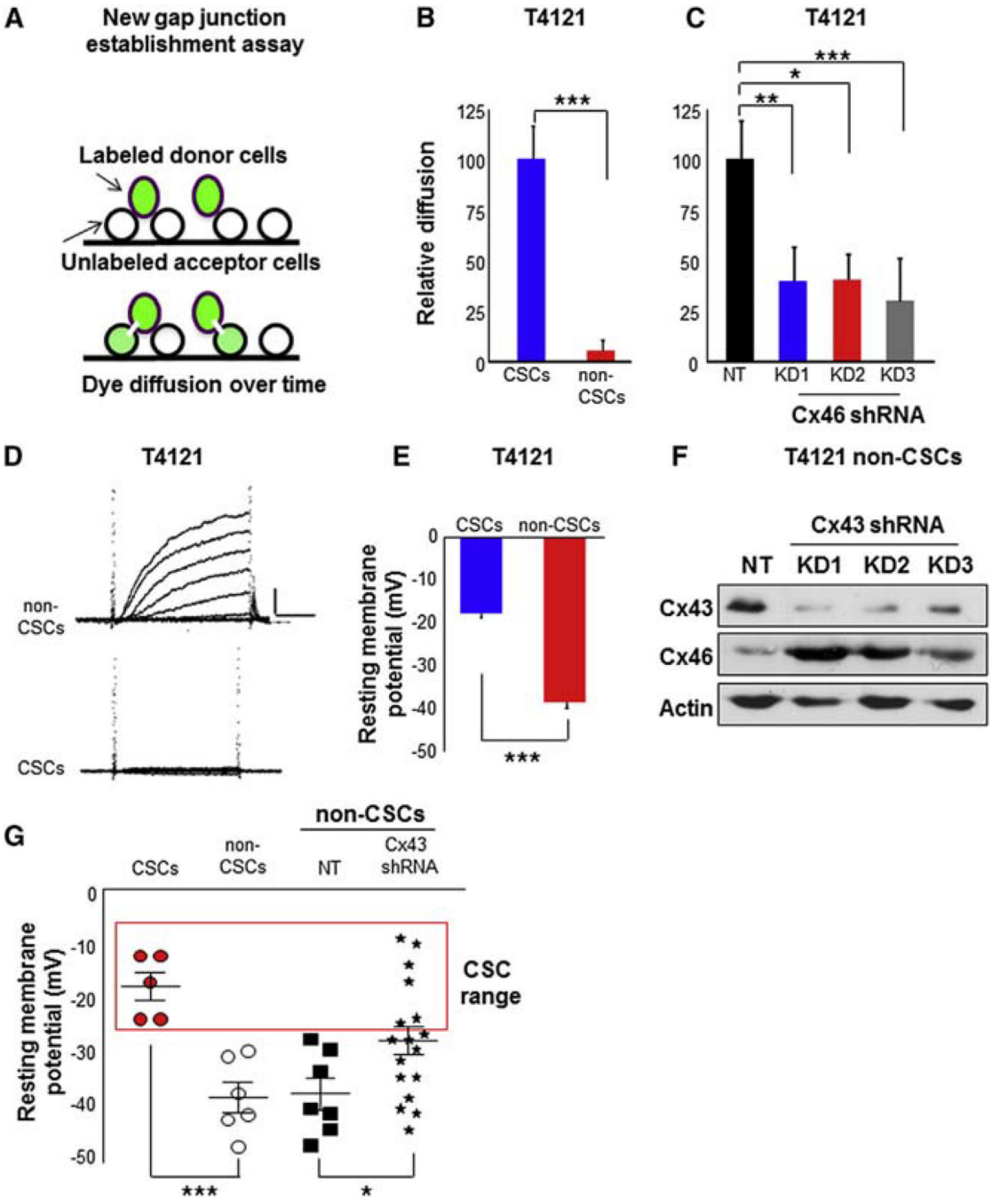

Figure 5. CSCs and Non-CSCs Express Different Connexins that Facilitate Differential Rates of Cell-Cell Communication and Resting Membrane Potential

(A) Schematic depicts assay to evaluate the formation of new gap junctions in which the dye diffuses to unlabeled cells upon the establishment of gap junctions.

(B) Relative diffusion after 8 hr differs between CSCs and non-CSCs derived from the T4121 GBM xenograft.

(C) After Cx46 KD, relative diffusion is significantly reduced compared with the NT control.

(D) Electrophysiological analysis of the outward currents recorded in CSCs and non-CSCs demonstrates a reduction in CSC currents compared with non-CSCs.
(E and F) Voltage-clamp analysis (E) demonstrates that the resting membrane potential of CSCs is higher than that of non-CSCs. Cx43 was depleted by lentiviral delivery of shRNA using non-overlapping constructs against different parts of the gene, and representative immunoblots from non-CSCs derived from xenograft T4121 (F) demonstrate that Cx43 KD increased Cx46 expression compared with the NT control. Similar results were obtained in T387 (data not shown).
(G) Summary graph of voltage-clamp analysis demonstrates that the resting membrane potential of CSCs was higher than that of non-CSCs. Cx43 KD in non-CSCs resulted in an increase in resting membrane potential. Red box indicates resting membrane potential range of CSCs.
Data in graphs represent mean values ± SD; *$p < 0.05$, **$p < 0.01$, ***$p < 0.001$ as assessed by one-way ANOVA. Current traces were plotted every 20 mV for clarity, and the calibration bar represents 2.5 ms and 5 pA/pF.

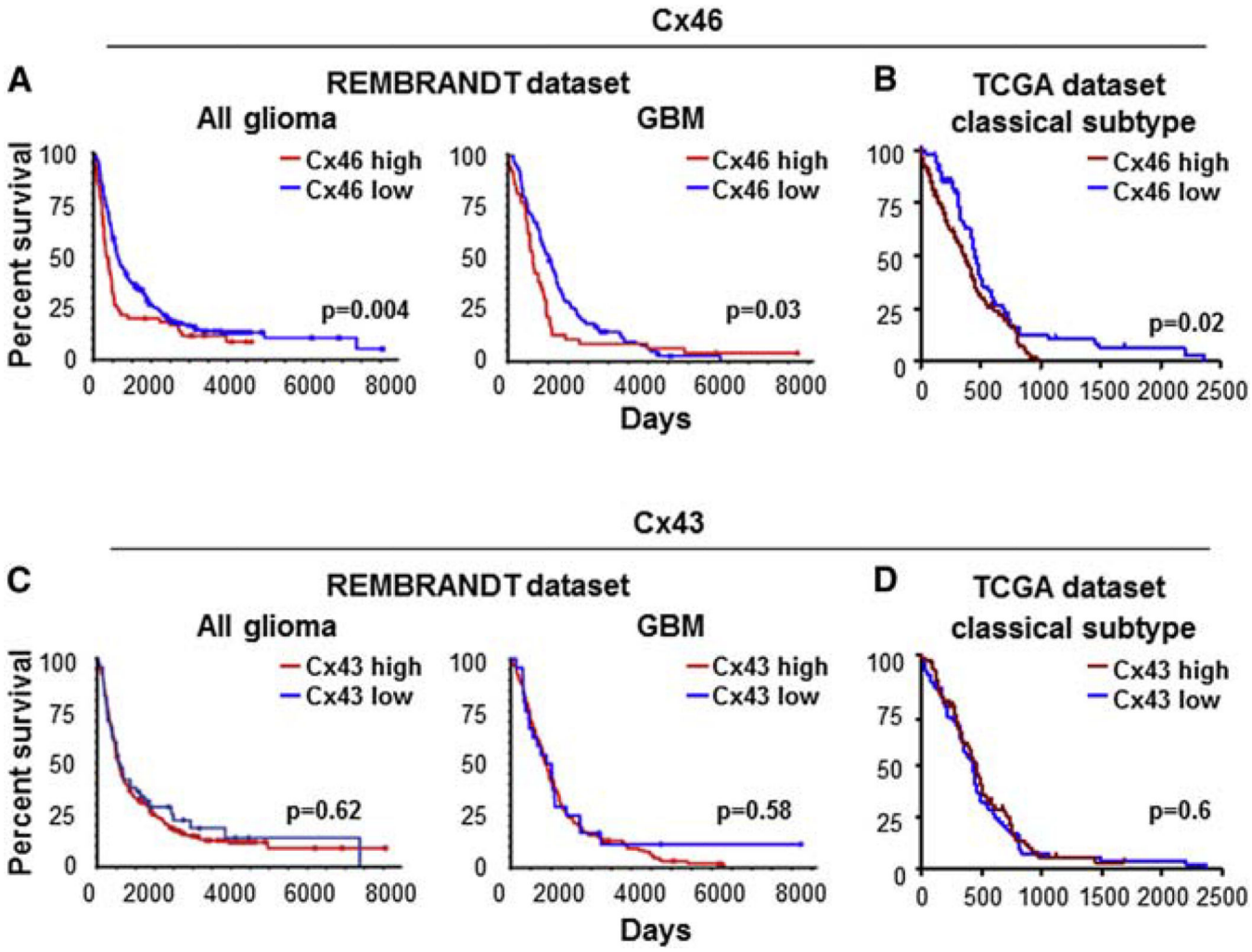

Figure 6. Bioinformatics Analysis of Cell Junction Proteins Reveals a Negative Correlation between Cx46 and GBM Patient Survival

(A and B) Cx46 negatively correlated with overall glioma and GBM patient survival as assessed by the NCIREM BRANDT database (A) and with GBM patient survival in TCGA classical molecular subtype (B).

(C and D) Cx43 did not correlate with overallglioma or GBM patient survival as assessed by the NCI REM BRANDT database (C) or with GBM patient survival in TCGA classical molecular subtype (D). Statistical assessments were performed using log rank survival analysis and p values are indicated directly on survival plots.

See also Figure S3.